EVALUATION OF A DYNAMIC LES MODEL FOR THE COMPUTATION OF FREE SHEAR FLOWS USING A HIGH-ORDER NUMERICAL METHOD.

J.-B. Chapelier
Purdue University, School of Mechanical Engineering, West Lafayette, Indiana, USA
jchapeli@purdue.edu

G. Lodato
Normandie Université, CNRS, INSA et Université de Rouen, CORIA UMR6614
guido.lodato@insa-rouen.fr

Abstract

A dynamic model for Large-Eddy Simulation (LES) suitable for discontinuous finite element methods is validated in the context of free shear flows. The main feature of the model is a turbulence sensor built from the evaluation of the modal energy spectrum in each element of the discretization. The evaluation of the sharpness of the energy decay in each element allows to locally identify the under-resolution and adapt accordingly the intensity of the sub-grid dissipation. The present approach is tested on the LES of the temporally developing mixing layer at $Re = 500$ for assessing the proposed model to represent accurately the transition and the coherent vortices. It is found that the model leads to an accurate description of transitional vortical flows at coarse resolutions. It is also found to provide accurate results on distorted grids while maintaining the computations robust.

Introduction

Discontinuous finite element methods (DFEM) such as the Discontinuous Galerkin (DG) or Spectral Difference (SD) methods (see Cockburn *et al.*, 2000; Kopriva & Kolias, 1996; Liu *et al.*, 2006; Wang *et al.*, 2007) show a strong potential for the simulation of turbulence on complex geometries by the means of DNS or LES due to their high-orders of accuracy, the ability to handle unstructured meshes, curved elements and the compactness of the stencil which allows for a good parallel efficiency.

DFEM naturally introduce a numerical dissipation originating from the upwinding of the numerical flux computed at the cell interfaces. The numerical dissipation has been studied in the context of canonical turbulent flows Chapelier *et al.* (2016*b*,*a*) and it has been found that this dissipation alone is not sufficient to provide an accurate description of high Reynolds turbulent flows on coarse grids. Dissipative SGS models are therefore needed to complement this numerical dissipation in order to obtain physically consistent results for high-Reynolds, under-resolved turbulent flows computations.

The semi-local nature of DFEM approaches (a spectral representation of the solution in each of the discretization cell) offers many possibilities for turbulence modeling. In particular, the modal decomposition of the signal in each cell allows for evaluating local spectra which can be used for various modeling approaches. For example, it allows for an easy implementation of multi-scale LES models, such as the VMS introduced by Hughes *et al.* (2001). In the present work, a new dynamic LES model is proposed by blending ingredients from existing dynamic turbulence models and modal shock capturing techniques based on the polynomial scale decomposition of the signal. In particular, Persson & Peraire (2006) and Klöckner *et al.* (2011) proposed shock sensors built on the modal decay of the density component allowing for the identification of cells in which a shock is present. In Chapelier & Lodato (2016), this idea has been extended for the detection of under-resolved regions for the LES of turbulent flows. This new approach has been found to provide an accurate, robust and easy to implement LES modeling strategy for DFEM, in the context of canonical turbulence. In the present work, this model is further assessed in the context of free shear flows. A temporal mixing layer configuration is considered and the DFEM results compared to state of the art LES computations. The influence of the order of accuracy and grid distortion on the solution quality is also assessed for this configuration.

1 Methodology

The SD method is considered for the resolution of the compressible Navier-Stokes equations on unstructured meshes. All the details for the implementation can be found in the work of Lodato *et al.* (2013). This method features an arbitrary high-order spatial discretization with upwind fluxes (based on the Roe scheme) for the inviscid terms and centered fluxes for the viscous terms. The approach is compact, handles unstructured and curved mesh elements and is scalable for thousands of computational cores in the case of parallel computations.

In Chapelier & Lodato (2016), a new dynamic approach for LES—called SEDM—that accounts for the embedded numerical dissipation of the SD scheme has been developed and validated in the context of fundamental turbulence test cases. The main feature of this dynamic model is its ability to detect under-resolution at the cell level and adapt the intensity of the sub-grid dissipation accordingly.

The development of the SEDM follows three different steps. The first step consists in building a turbulence sensor able to discriminate between (well-resolved) laminar and (under-resolved) turbulent regions. This sensor is based on the evaluation of the spectral energy decay which provides a powerful indicator to detect the presence of well- or under-resolved turbulence. DFEM allow for a cell-local evaluation of the energy decay which leads to the validity of such a sensor for unstructured meshes. The one-dimensional energy spectrum in each cell can be obtained by computing the modes of the velocity components corresponding to a hierarchical polynomial basis. In this case, the energy spectra read:

$$E^j(k) = [V_{kl} u(\xi_l)]^2, \tag{1}$$

where u is a component of the velocity vector, $V_{kl} = L_k(\xi_l)$ is the Vandermonde matrix, L_k the basis of Legendre polynomials and k the number of the Legendre mode. The modal energy decay can then be evaluated, for example, by assuming that the energy spectrum follows a power law $E^j(k) \propto k^{-\sigma_j}$, where σ_j is the power decay of the spectrum in the cell j. The values of σ_j can be computed using a least-square fit. High values of σ_j characterize a fast decay of energy in the cell, which typically corresponds to well-resolved or laminar regions in which the small-scale energy is low. Low values of σ_j correspond to under-resolved regions with highly-energetic small-scales and the possible presence of high-frequency numerical oscillations.

The next step consists in defining a function $f(\sigma_j)$ which lowers the intensity of the sub-grid stresses in well-resolved regions. The following expression guarantees a smooth transition of the sub-grid dissipation intensity between the well- and under-resolved regions of the flow:

$$f(\sigma_j) = \begin{cases} 0 & \text{if } \sigma_j > \sigma_t + 2\kappa, \\ 1 & \text{if } \sigma_j < \sigma_t, \\ \frac{1}{2} + \frac{1}{2}\sin\left(\pi \frac{\sigma_t + \kappa - \sigma_j}{2\kappa}\right) & \text{elsewhere,} \end{cases} \tag{2}$$

where σ_t is the value of σ_j defining the limit of under-resolution and κ is a parameter defining the sharpness of the function f.

The last step consists in defining the expression of the eddy viscosity. A mean eddy viscosity is first built in each cell:

$$\nu_t^j = C_{\text{SEDM}}^2 f(\sigma_j) \Delta_j \sqrt{k_j}, \quad j = 1, \ldots, N_{\text{el}}, \tag{3}$$

where k_j is the mean turbulent kinetic energy in the element j and $\Delta^j = \Delta_x^j/(p+1)$ the cutoff length. A continuous spatial variation of ν_t is recovered by computing the mean values of the viscosity at the element vertices. The eddy viscosity is therefore assumed to be piece-wise linear within each element. The parameters $C_{\text{SEDM}} = 0.23$ and $\sigma_t = 1.6$ have been calibrated from *a priori* studies of a DNS of isotropic turbulence (Chapelier & Lodato, 2016). The value of $\sigma_t = 1.6$ is not expected to vary because of the universality of scales located in the inertial range which, in turn, guarantee a constant power decay at high Reynolds numbers. The parameter $C_{\text{SEDM}} = 0.23$ is defined so that the maximum level of sub-grid dissipation is sufficient in a very high Reynolds number configuration. The SEDM approach will ensure that the sub-grid dissipation is lowered in well-resolved, transitional or laminar regions of the flow. The parameter κ is set to 0.3 for the following tests, as proposed in the work of Chapelier & Lodato (2016) in which a sensitivity study of this parameter was performed.

2 Mixing Layer computations

The accuracy of the SEDM approach is assessed for a temporal mixing layer flow configuration. The flow setup corresponds to the configuration considered by Vreman *et al.* (1997). The computational domain $\Omega = [0, L] \times [-L/2, L/2] \times [0, L]$ is cubic with periodic boundary conditions in the longitudinal and transversal directions. L is the domain length corresponding to about eight times the dominant wavelength. Wall-slip conditions are imposed at the boundaries in the shear-layer direction. The shear layer is defined by imposing the following initial velocity profile:

$$u = \frac{(U_1 - U_2)}{2} \tanh(y), \quad v = 0, \quad w = 0, \tag{4}$$

where U_1 and U_2 are the upper and lower stream velocities, respectively. The component u is perturbed by a random noise of amplitude 0.05 in order to trigger the transition to turbulence. The Reynolds number based on the upper stream velocity and initial vorticity thickness is set to 500. The upper stream Mach number is set to 0.2. In the present study, the accuracy of the SEDM approach is compared to the state of the art LES computation of Vreman *et al.* (1997). This reference computation features a 120^3 grid and is explicitly filtered using a filter length corresponding to a 60^3 grid in order to remove the influence of the numerical errors related to the discretization; the dynamic model of Germano *et al.* (1991) was adopted to model the sub-grid scale stresses. The SEDM computation considered using the SD method features an eighth order of accuracy (equivalent to a polynomial degree $p = 7$) and 8^3 elements leading to a total of 64^3 degrees of freedom (DoF). It is interesting to note that, for this particular SD discretization, the computation without sub-grid model becomes unstable during the mixing layer growth. The number of DoF of the SD discretization is reduced by a factor 7 when compared to the reference computation of Vreman *et al.* due to the absence of explicit filtering. As seen from Figures 1,2 and 3, the SEDM computation compares very well with the reference computation in terms of the evolution of the momentum thickness and the longitudinal Reynolds stresses at two different times. Figures 4,5 and 6, which present the Q criterion iso-surfaces at three different times, show well-defined vortical structures with the presence of small-scale turbulence during the late stages of the computation. In terms of computational costs, it is expected that the current methodology is more efficient compared to the reference, explicitly filtered, Dynamic model computation. First, for the reference computation of Vreman *et al.*, the explicit filter of the solution reduces the actual effectiveness of the computational grid, as only 60^3 DoFs become relevant over the 120^3 DoFs grid. Although we can argue that this explicit filter removes the numerical errors, the SEDM computation keeps all DoFs effective, therefore inducing a consequent reduction in terms of computational cost. Second, the Dynamic model involves a number of test

filtering and averaging to determine the dynamic parameter, while the SEDM approach has been shown to be almost equivalent to the Smagorinsky model in terms of computational cost (Chapelier & Lodato, 2016).

Sixth order accurate SD computations are considered as well to explore the influence of the order of accuracy on the quality of the solution. The sixth order discretization features a polynomial degree $p = 5$ and 16^3 mesh elements leading to the definition of 96^3 degrees of freedom. The sixth order computation is run using the SEDM approach. The longitudinal Reynolds stresses are plotted at times $t = 160$ and $t = 200$ for the 6th order computations in Figures 7 and 8, and the results are compared to the 8th order SEDM computation and the reference computation by Vreman *et al.*. The sixth order SEDM computation shows a good agreement with the reference results of Vreman, and the profiles are also close to the 8th order SEDM computation. The interest of increasing the order of accuracy is clearly demonstrated in these pictures 7 and 8, as the 8th order SEDM computation shows a lower number of degrees of freedom than the 6th order counterpart for similar results.

The last computations involve comparisons between regular and distorted meshes. The sixth order regular mesh is taken as reference and the position of the element vertices randomly moved in all directions by a length $0.2h$ where $h = 120/16$ is the element size for the regular mesh. The resulting mesh is shown in Figure 9. A sixth order SEDM computation is run using this mesh and the results compared to the regular mesh computation. Figures 10 and 11 show the longitudinal Reynolds stresses at times $t = 160$ and $t = 200$ for the computation on the regular and distorted grids. At $t = 160$, there is almost no difference between the Reynolds stresses on the regular and distorted grid. At $t = 200$, the distorted grid computation leads to a slight overestimate of the turbulent energy at the center of the computational domain. However, the overall trend is similar for both computations, which shows that the present methodology is robust for computations on distorted grids.

Conclusion

A new dynamic LES model suitable for DFEM has been validated in the context of free shear flows. Its main feature is a local turbulence sensor built from the evaluation of the decay of the modal energy in each of the discretization elements. This approach has been applied successfully for LES computations of the temporally developing mixing layer using the SD method. The combination of a high-order of accuracy with an accurate sub-grid model leads to results which are similar to an explicitly filtered LES, which is much more expensive in terms of resolution. In particular, the same quantitative agreement, for the mixing layer growth rate and fluctuating velocity profiles, is found between a eighth order SEDM computation with 64^3 DoF and the explicitly filtered LES with 120^3 DoF. Different polynomial orders have been assessed, and it is found that the SEDM benefits from higher-orders as more degrees of freedom are necessary to obtain a quantitatively similar result for lower orders. The approach has also been found to be robust to grid distortion, as computations on randomly deformed meshes lead to the same qualitative agreement as computations performed on regular Cartesian grids. Future work will aim at assessing the present methodology for more complex configurations and flow physics, such as separated or compressible flows.

REFERENCES

Chapelier, Jean-Baptiste, De La Llave Plata, Marta & Lamballais, Eric 2016*a* Development of a multiscale LES model in the context of a modal discontinuous Galerkin method. *Comput. Meth. Appl. Math. Eng.* **307**, 275–299.

Chapelier, J.-B. & Lodato, G. 2016 A spectral-element dynamic model for the large-eddy simulation of turbulent flows. *J. Comput. Phys.* **321**, 279–302.

Chapelier, Jean-Baptiste, Lodato, Guido & Jameson, Antony 2016*b* A study on the numerical dissipation of the Spectral Difference method for freely decaying and wall-bounded turbulence. *Comp. Fluids* **139**, 261–280.

Cockburn, B., Karniadakis, G.E. & Shu, C.W. 2000 Discontinuous Galerkin methods: Theory, Computation, and Applications, volume 11 of lecture notes in computational science and engineering.

Germano, M., Piomelli, U., Moin, P. & Cabot, W.H. 1991 A dynamic subgrid-scale eddy viscosity model. *Phys. Fluids* **3** (7), 1760–1765.

Hughes, T.J.R., Mazzei, L., Oberai, A.A. & Wray, A.A. 2001 The multiscale formulation of Large-Eddy Simulation: Decay of homogeneous isotropic turbulence. *Phys. Fluids* **13**, 505.

Klöckner, Andreas, Warburton, Tim & Hesthaven, Jan S 2011 Viscous shock capturing in a time-explicit discontinuous Galerkin method. *Math. Model. Nat. Phenom.* **6** (03), 57–83.

Kopriva, David A & Kolias, John H 1996 A conservative staggered-grid Chebyshev multidomain method for compressible flows. *J. Comput. Phys.* **125** (1), 244–261.

Liu, Yen, Vinokur, Marcel & Wang, ZJ 2006 Spectral Difference method for unstructured grids I: basic formulation. *J. Comput. Phys.* **216** (2), 780–801.

Lodato, Guido, Castonguay, Patrice & Jameson, Antony 2013 Discrete filter operators for Large-Eddy simulation using high-order Spectral Difference methods. *Int. J. Numer. Meth. Fluids* **72** (2), 231–258.

Persson, Per-Olof & Peraire, Jaime 2006 Sub-cell shock capturing for discontinuous Galerkin methods. *AIAA paper* **112**, 2006.

Vreman, B, Geurts, Bernard & Kuerten, Hans 1997 Large-eddy simulation of the turbulent mixing layer. *J. Fluid Mech.* **339**, 357–390.

Wang, ZJ, Liu, Yen, May, Georg & Jameson, Antony 2007 Spectral Difference method for unstructured grids II: extension to the Euler equations. *J. Sci. Comput.* **32** (1), 45–71.

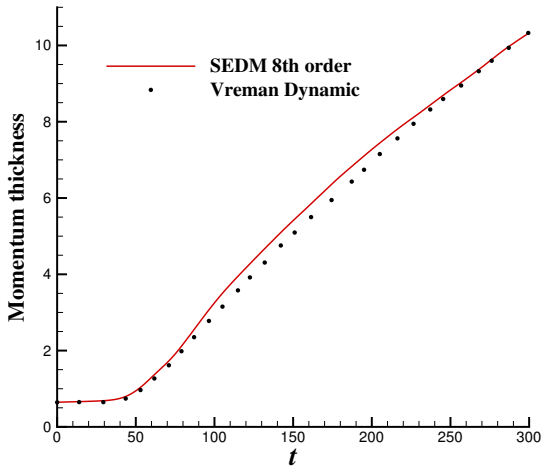

Figure 1. Evolution of the momentum thickness. 8th order SEDM computation.

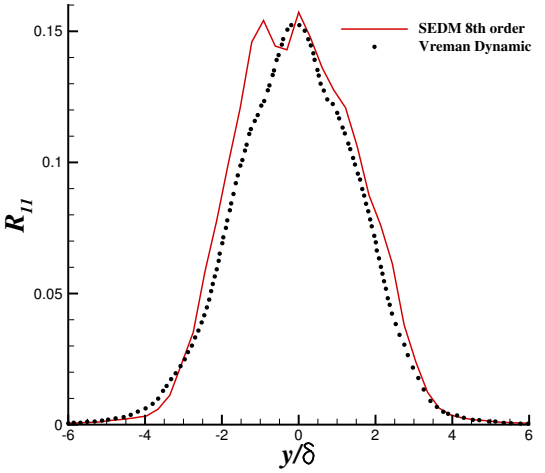

Figure 2. Longitudinal Reynolds stresses at $t = 160$. 8th order SEDM computation.

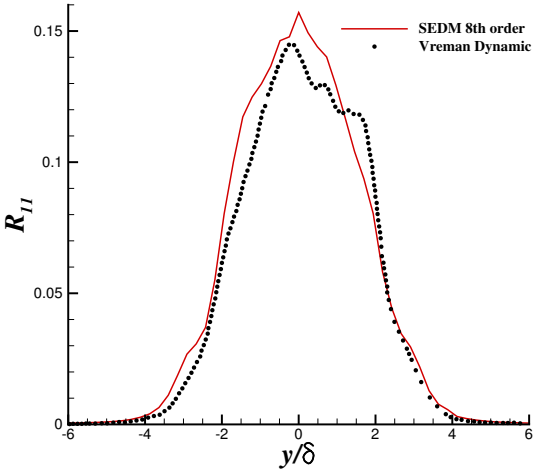

Figure 3. Longitudinal Reynolds stresses at $t = 200$. 8th order SEDM computation.

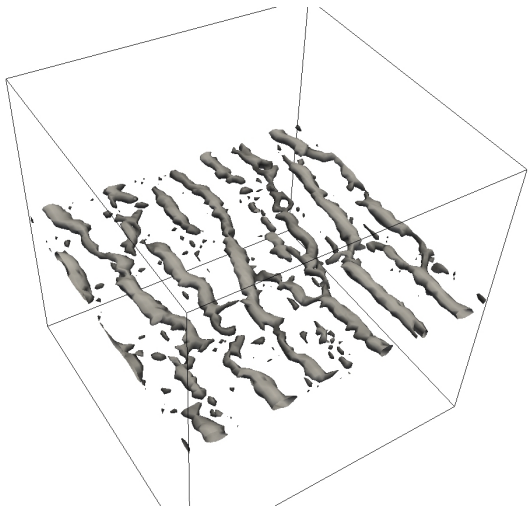

Figure 4. Q iso-surfaces at t=40 (8th order SEDM computation).

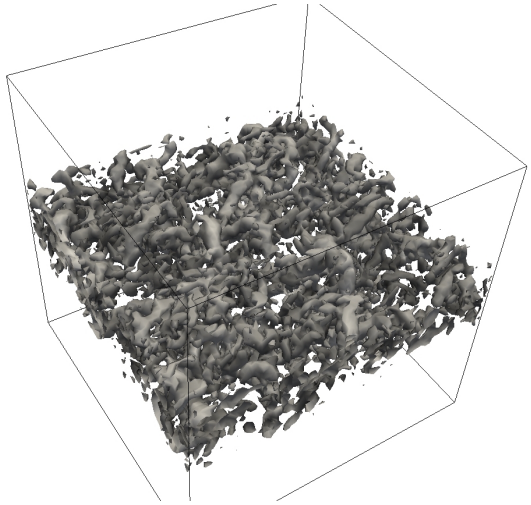

Figure 5. Q iso-surfaces at t=120 (8th order SEDM computation).

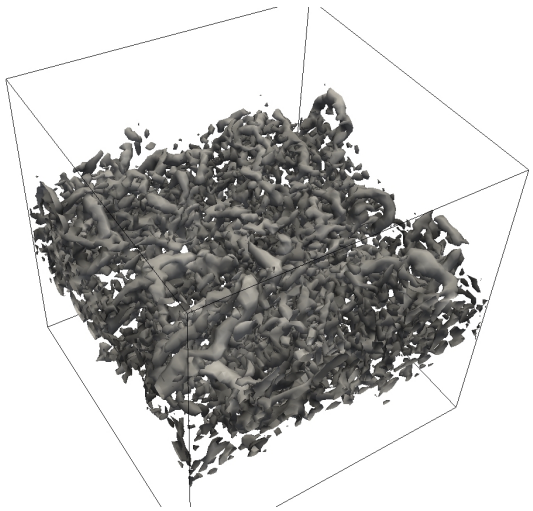

Figure 6. Q iso-surfaces at t=200 (8th order SEDM computation).

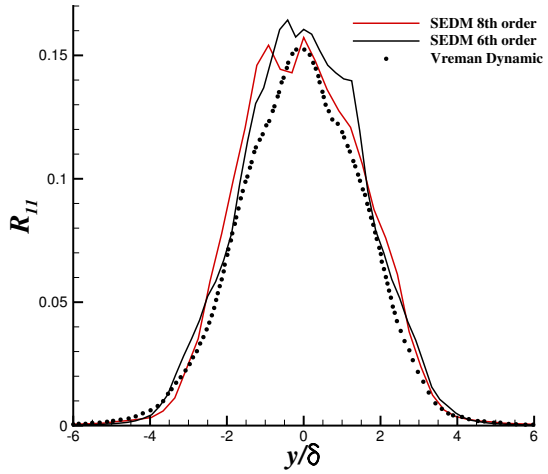

Figure 7. Longitudinal Reynolds stresses at $t = 160$, 6th order computations.

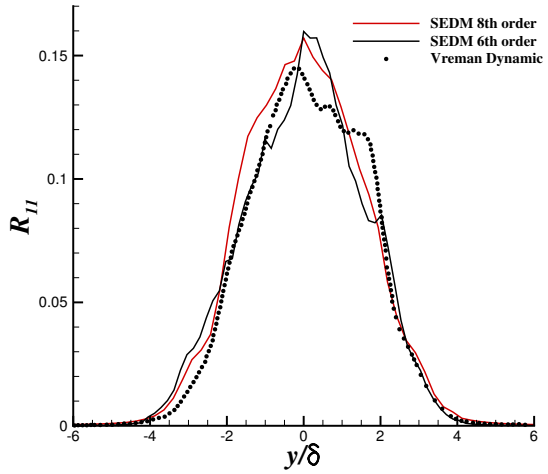

Figure 8. Longitudinal Reynolds stresses at $t = 200$, 6th order computations.

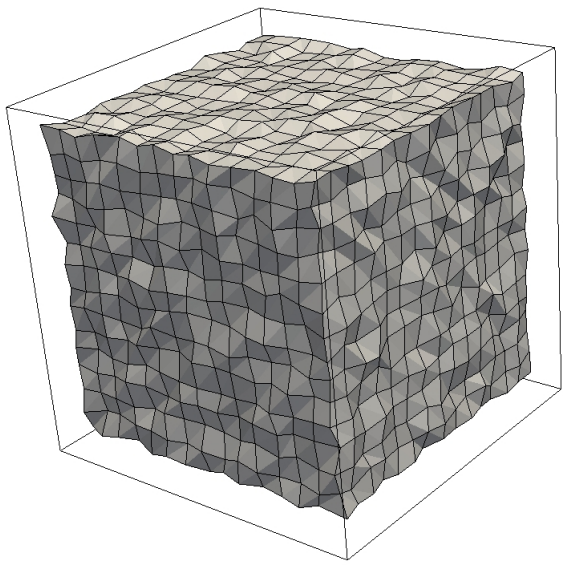

Figure 9. Sketch of the distorted mesh used for the sixth order SEDM mixing layer computation.

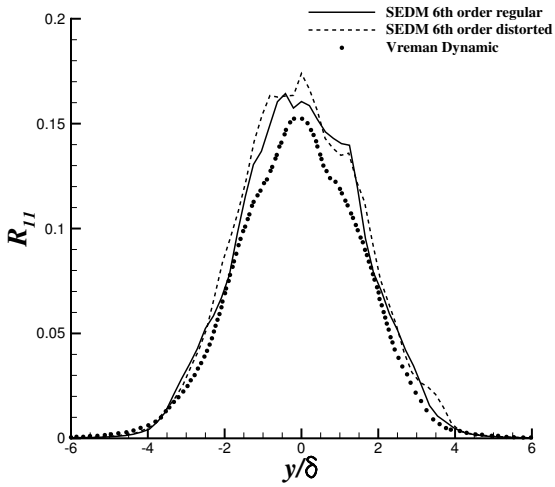

Figure 10. Longitudinal Reynolds stresses at $t = 160$, 6th order computations, comparison between regular and distorted mesh.

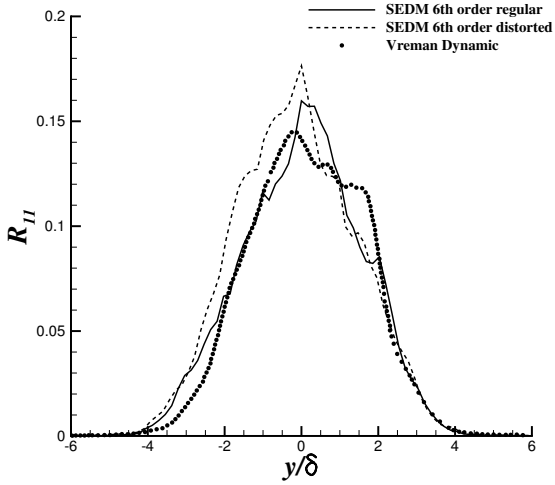

Figure 11. Longitudinal Reynolds stresses at $t = 200$, 6th order computations, comparison between regular and distorted mesh.